Iterative method to improve the precision of the quantum-phase-estimation algorithm

Junxu Li ⬤ *

Department of Physics, College of Science, Northeastern University, Shenyang 110819, China

Here we revisit the quantum-phase-estimation (QPE) algorithm and devise an iterative method to improve the precision of QPE with propagators over a variety of time spans. For a given propagator and a certain eigenstate as input, QPE with a propagator is introduced to estimate the phase corresponding to an eigenenergy. Due to the periodicity of the complex exponential, we can pinpoint the eigenenergy in a branch of comblike ranges by applying QPE with propagators over longer time spans. Thus, by picking up appropriate time spans, the iterative QPE with corresponding propagators can enable us to pinpoint the eigenenergy more precisely. Moreover, even if there are only a few qubits as ancilla qubits, high precision is still available by the proposed iterative method. Our work provides a feasible and promising means toward precise estimations of an eigenvalue on noisy intermediate-scale quantum devices.

I. INTRODUCTION

In 1982, Feynman proposed that quantum mechanical devices could perform computation [1]. Since then, interest in quantum computing has grown enormously. Quantum computers are expected to solve the classically intractable problems, ranging from integer factorization to simulating many-body quantum physics. Recent developments in quantum hardware have demonstrated the dawn of "quantum supremacy" [2–6]. These key results motivate researchers to revisit and develop quantum algorithms [7–11].

In this context, the quantum-phase-estimation (QPE) algorithm, first introduced by Kitaev in 1995 [12] to estimate the phase corresponding to an eigenvalue of a given unitary operator, might be one of the most famous and powerful quantum algorithms. QPE is also the critical subroutine in a variety of quantum algorithms, including Shor's algorithm [13] and Harrow-Hassidim-Lloyd algorithm [14]. Moreover, often combined with adiabatic state preparation [15], QPE is also a powerful tool for chemists solving electronic structure problems, where QPE is implemented to estimate the ground energy of atoms and small molecules with a given Hamiltonian [11,16–20]. However, QPE requires deep circuits with ancilla qubits [21], which are hard to execute in a noisy intermediate-scale quantum (NISQ) era [22] with limited quantum resources. For example, in 2019, IBM researchers implemented QPE on the IBM QX quantum computer and reported that the accuracy and precision are severely constrained by the quantum devices' physical characteristics such as coherence time and error rates [23]. Therefore, a feasible approach to improve the precision of QPE is of great demand in the NISQ era.

In this paper, we revisit the typical QPE and devise an iterative method to improve the precision. We will show that the QPE with propagators over longer time spans can lead to comblike ranges in the estimation due to the periodicity of the complex phase. Therefore, by implementing various propagators over appropriate time spans, the iterative QPE is capable to pinpoint the eigenenergy more precisely. In the standard QPE algorithm, precision is gained by adding more qubits. In the proposed iterative method, precision is gained in each iteration, even with only a few ancilla qubits. Our work provides a feasible and promising means toward precise estimations of an eigenvalue on NISQ devices. An outline for the rest of the paper is as follows. In Sec. II, we provide a brief overview of the implementation of propagators on a quantum computer. In Sec. III, we revisit how QPE with propagators can be applied to solve the eigenvalue problem. Then, in Sec. IV, we present the iterative method to improve the precision of QPE with propagators, and in Sec. V, a simple example is presented. Finally, we give our discussion and concluding remarks in Sec. VI.

II. FROM PROPAGATORS TO UNITARY OPERATORS

For a given Hamiltonian H, the propagator describing the evolution from t_{in} to t_f can be written as

$$K(t_f; t_{in}) = \exp[iH(t_f - t_{in})]. \tag{1}$$

A general construction of the quantum circuit to simulate the propagator is performed as follows [24]. Initially, prepare H as a sum over products of Pauli spin operators by the Jordan-Wigner transformation [25,26]. Next, H can be compiled into fundamental gates by using Trotter-Suzuki formulas [27], where the complicated Hamiltonian is complied as a sum of solvable ones. Denote their sequential implementation on a quantum computer as $U_K(t_f; t_{in})$, which can be made to approximate the unitary propagator $K(t_f; t_{in})$.
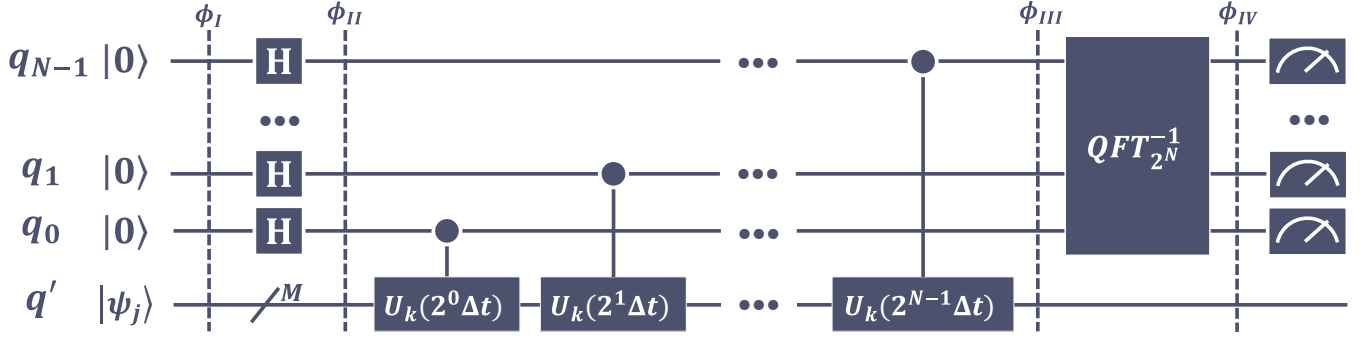
*lijunxu1996@gmail.com

FIG. 1. Schematic diagram of the QPE circuit with propagators. There are two registers, with the first N qubits initialized at ground state $|0\rangle$, and the others prepared at the jth eigenstate $|\psi_j\rangle$. At the beginning, Hadamard gates are applied on $q_0, \cdot, q_{N-1}$ to convert the first register into a uniform superposition. The succeeding controlled gates then prepare a superposition of the evolution. Next, the inverse quantum Fourier transform is applied on the first register. By the end, measurements are applied on the first register. We annotate the states at various stage as $\phi_I, \ldots, \phi_{IV}$, as indicated by the dashed line.

The nonrelativistic propagator can also be obtained in path integral formulation [28],

$$K(x_f, t_f; x_{in}, t_{in}) = \int_{x_{in}}^{x_f} \exp(iS[x])\mathcal{D}x, \quad (2)$$

where $S[x]$ denotes the action and $\mathcal{D}x$ denotes the integration over all paths.

If the initial wave function Ψ_{in} is known, the new wave function Ψ_f can be derived with the propagator,

$$\Psi_f(x_f, t_f) = \int K(x_f, t_f; x_{in}, t_{in})\Psi_{in}(x_{in}, t_{in})dx_{in}, \quad (3)$$

where the initial time t_{in} and final time t_f are fixed. Recall that the propagator can also be written as

$$K(x_f, t_f; x_{in}, t_{in}) = \sum_n |\psi_n\rangle\langle\psi_n|e^{-iE_n(t_f-t_{in})/\hbar}, \quad (4)$$

where ψ_n is the nth eigenstate corresponding to eigenenergy E_n. Thereafter, the corresponding operator U_K can be decomposed as

$$U_K(t_f; t_{in}) = T^\dagger U_E T, \quad (5)$$

where $U_E = \sum_n |n\rangle\langle n|e^{iE_n(t_f-t_{in})/\hbar}$ is a diagonalized unitary operator, and T is a unitary transformation from the eigenstate basis to the computational basis. In quantum simulation, the propagator can be efficiently carried out using Trotter decomposition [27], provided that the Hamiltonian can be decomposed into a sum of local ones [29].

III. QUANTUM-PHASE-ESTIMATION ALGORITHM WITH PROPAGATORS

The QPE with propagators is similar to the original QPE, where the given unitary operator U is replaced by operator U_K that approximates the propagator.

Our goal is to estimate the phase corresponding to an eigenvalue of the given propagator. In Fig. 1, we present a schematic diagram of the QPE circuit with propagator. There are two registers, the first N qubits are denoted as q and the others are denoted as q'. The q qubits are initialized at

ground state $|0\rangle$, and the q' qubits are prepared at $|\psi_j\rangle$, which is the jth eigenstate corresponding to eigenenergy E_j. For simplicity, in the following discussion, we denote $U_K(\Delta t) = U_K(t_{in} + \Delta t; t_{in})$.

At the very beginning, the overall quantum state is

$$|\Phi_I\rangle = |0\rangle^{\otimes N} \otimes |\psi_j\rangle. \quad (6)$$

Next, N Hadamard gates prepare a uniform superposition, and the quantum state at stage II is

$$|\Phi_{II}\rangle = \frac{1}{2^{N/2}} \sum_{n=0}^{2^N-1} |n\rangle \otimes |\psi_j\rangle. \quad (7)$$

The succeeding controlled gates prepare a superposition of the evolution, and the overall quantum state at stage III is

$$|\Phi_{III}\rangle = \frac{1}{2^{N/2}} \sum_{n=0}^{2^N-1} |n\rangle \otimes U_K(n\Delta t)|\psi_j\rangle. \quad (8)$$

Recalling that $U_K(\Delta t)|\psi_j\rangle = e^{-iE_j\Delta t/\hbar}|\psi_j\rangle$, we have

$$|\Phi_{III}\rangle = \frac{1}{2^{N/2}} \sum_{n=0}^{2^N-1} (|n\rangle \otimes e^{-iE_j n\Delta t/\hbar}|\psi_j\rangle). \quad (9)$$

Then, quantum Fourier transform (QFT) is applied on the first N qubits,

$$|\Phi_{IV}\rangle = \frac{1}{2^N} \sum_{x,n=0}^{2^N-1} (e^{2\pi inx/2^N}|x\rangle \otimes e^{-iE_j n\Delta t/\hbar}|\psi_j\rangle)$$

$$= \frac{1}{2^N} \sum_{x,n=0}^{2^N-1} (e^{2\pi inx/2^N - iE_j n\Delta t/\hbar}|x\rangle \otimes |\psi_j\rangle). \quad (10)$$

Notice that if $2\pi x/2^N = E_j\Delta t/\hbar$ exactly,

$$\frac{1}{2^N} \sum_{n=0}^{2^N-1} e^{2\pi inx/2^N - iE_j n\Delta t/\hbar} = 1. \quad (11)$$

Otherwise, we have

$$\frac{1}{2^N} \sum_{n=0}^{2^N-1} e^{2\pi inx/2^N - iE_j n\Delta t/\hbar} = \frac{1}{2^N} \frac{1 - e^{i(2\pi x - 2^N E_j \Delta t/\hbar)}}{1 - e^{i(2\pi x/2^N - E_j \Delta t/\hbar)}}. \quad (12)$$

In brief, if $2^N E_j \Delta t/2\pi\hbar$ is exactly an integer, the probability to get result $|x\rangle$ after measuring the first N qubits is

$$Pr(x) = \begin{cases} 1, & x = \frac{2^N E_j \Delta t}{2\pi\hbar} \\ 0, & x \neq \frac{2^N E_j \Delta t}{2\pi\hbar}. \end{cases} \quad (13)$$

On the other hand, if $2^N E_j \Delta t/2\pi\hbar$ is not an integer, then we have

$$Pr(x) = \left| \frac{1}{2^N} \frac{1 - e^{i(2\pi x - 2^N E_j \Delta t/\hbar)}}{1 - e^{i(2\pi x/2^N - E_j \Delta t/\hbar)}} \right|^2. \quad (14)$$

Therefore, the highest probability outcome is the integer value y closest to the E_j phase term. Integer y ensures that $|y/2^N - E_j \Delta t/2\pi\hbar| \leqslant 1/2^{N+1}$, and it is proven that $\Pr(y) \geqslant 4/\pi^2$ [30]. Theoretically, by measuring all q qubits after applying the QPE algorithm, we can pinpoint $E_j \Delta t/2\pi\hbar$ in a certain slot $[(y_j - 1/2)/2^N, (y_j + 1/2)/2^N]$, where $0 \leqslant y_j < 2^N - 1$ is the nearest integer corresponding to the greatest probability $\Pr(y_j)$. The algorithm must be run many times to collect enough data to identify the correct peak in the sampled distribution.

IV. AN ITERATIVE METHOD TO IMPROVE THE PRECISION

The inclusion of propagators enables an iterative method to improve the precision of QPE. In the following discussion, we assume that the QPE is always accurate as expected. Yet due to the existence of noises and errors, the measurement results of QPE might not peak at a single slim slot. Instead, it often occurs that there is a plateau that covers several slots. In this regard, we only need to replace the single slot with the range of the plateau, and the iterative method still works.

Consider the jth eigenstate $|\psi_j\rangle$ as input; by performing the QPE with propagator $U_K(\Delta t)$, we can pinpoint the phase term $E_j \Delta t/2\pi\hbar$ in a certain slot,

$$\frac{E_j \Delta t}{2\pi\hbar} \in \left[\frac{y_j - 1/2}{2^N}, \frac{y_j + 1/2}{2^N} \right], \quad (15)$$

where $0 \leqslant y_j < 2^N - 1$ is the nearest integer. For simplicity, here we assume that $\Delta t \leqslant 2\pi\hbar/E_j$ and $E_j > 0$, which ensures $E_j \Delta t/2\pi\hbar \in [0, 1]$.

Similarly, if we apply the QPE with propagator over a longer time span $U_K(\alpha\Delta t)$, we can pinpoint $\alpha E_j \Delta t/2\pi\hbar$ in slot $[y_j(\alpha)/2^N, (y_j(\alpha) + 1)/2^N]$, where $\alpha > 1$, and $0 \leqslant y_j(\alpha) < 2^N - 1$ is the corresponding nearest integer. In Fig. 2, we present a schematic diagram of the estimation. As shown in Fig. 2(a), the estimated $E_j \Delta t/2\pi\hbar$ is pinpointed in the stripe colored in navy, whose width is $1/2^N$. Similarly, QPE with propagator $U_K(\alpha\Delta t)$ informs that

$$\frac{\alpha}{2\pi}\left(\frac{E_j \Delta t}{\hbar} + 2k\pi \right) \in \left[\frac{y_j(\alpha) - 1/2}{2^N}, \frac{y_j(\alpha) + 1/2}{2^N} \right], \quad (16)$$
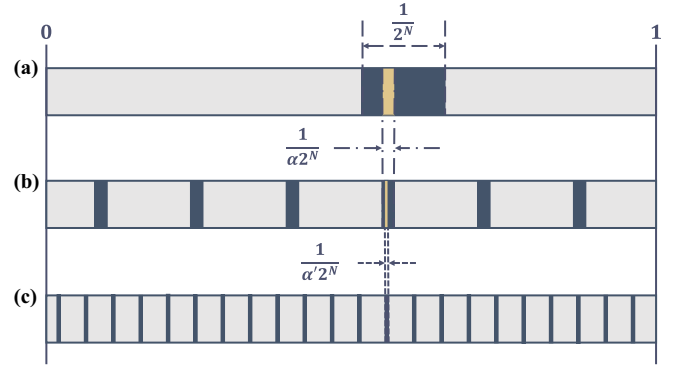

FIG. 2. Schematic diagram of the estimation $E_j \Delta t/2\pi\hbar$. The estimation is colored in navy. (a) The result of the QPE with propagator $U_K(\Delta t)$, where the estimation is located in a single stripe colored in navy, whose width is $1/2^N$. (b) The result of QPE with propagator $U_K(\alpha\Delta t)$; (c) QPE with propagator $U_K(\alpha'\Delta t)$. In (b) and (c), the estimated $E_j \Delta t/2\pi\hbar$ locates in a branch of narrower stripes. More precise estimation is achievable by studying the overlaps. The overlap of (a) and (b) is colored in yellow, shown in (a). The overlap of (a)–(c) is colored in yellow, shown in (b).

where $k \in Z$. Due to the periodicity of the complex exponential, Eq. (16) can be rewritten as

$$\frac{E_j \Delta t}{2\pi\hbar} \in \left[\frac{y_j(\alpha) - 1/2}{2^N \alpha} - \frac{k}{\alpha}, \frac{y_j(\alpha) + 1/2}{2^N \alpha} - \frac{k}{\alpha} \right]. \quad (17)$$

Equation (17) indicates that the same estimation of $E_j \Delta t/2\pi\hbar$ locates in a branch of narrow stripes as shown in Fig. 2(b), whose widths are $1/\alpha 2^N$. Notice that the exact value of k cannot be determined with Eq. (17) itself. Recalling Eq. (15), the estimated phase should also locate in a single stripe with width $1/2^N$, as shown in Fig. 2(a). Therefore, the k values can only be the integers ensuring that the intersection of Eqs. (15) and (17) is not empty. Then we can pinpoint the phase $E_j \Delta t/2\pi\hbar$ more precisely, which is the overlap of Eqs. (15) and (17). The overlap is colored in yellow, as depicted in Fig. 2(a).

Taking both Eqs. (15) and (17) into account, we are able to make a more precise estimation than using Eq. (15) itself. Yet we still need to find an optimal α value. Intuitively, a greater α value always leads to narrower stripes, as shown in Eq. (17). However, a greater α value also leads to closer neighbors [the distance between neighbors is $1/\alpha - 1/2^N \alpha$, according to Eq. (17)]. If there is more than one narrow stripe in the overlap, we can hardly exclude anyone from the final estimation. Aiming for a precise estimation, it should always be guaranteed that there is one and only one single stripe in the overlap. Therefore, we have to make a trade-off, as greater α leads to narrower slots but closer neighbors. Notice that if the distance between neighbors is no less than $1/2^N$, then there will be no more than one narrow stripe in the overlap. In other words, we need to ensure that

$$\frac{1}{\alpha} - \frac{1}{2^N \alpha} \geqslant \frac{1}{2^N}. \quad (18)$$

Thus the optimal choice is $\alpha = 2^N - 1$, with which we can pinpoint the phase in a single stripe whose width is

TABLE I. The optimal α values in iteration and the corresponding width of the corresponding estimation.

Iterative times	Optimal α	Width
0	1	$\frac{1}{2^N}$
1	$2^N - 1$	$\frac{1}{2^N(2^N-1)}$
2	$(2^N - 1)^2$	$\frac{1}{2^N(2^N-1)^2}$
...		
n	$(2^N - 1)^n$	$\frac{1}{2^N(2^N-1)^n}$

$1/2^N(2^N - 1)$,

$$\frac{E_j \Delta t}{2\pi \hbar} \in \left[\frac{y_j' - 1/2}{2^N(2^N - 1)}, \frac{y_j' + 1/2}{2^N(2^N - 1)} \right], \quad (19)$$

where $y_j' \leqslant 2^N(2^N - 1) - 1$ is the new nearest integer.

Moreover, higher precision is available by repeating the QPE with propagators and picking up appropriate α' values (here we use notation α' to avoid confusion). The QPE with propagator $U_K(\alpha' \Delta t)$ informs that

$$\frac{E_j \Delta t}{2\pi \hbar} \in \left[\frac{y_j(\alpha') - 1/2}{2^N \alpha'} - \frac{k'}{\alpha'}, \frac{y_j(\alpha') + 1/2}{2^N \alpha'} - \frac{k'}{\alpha'} \right], \quad (20)$$

where $k' \in \mathbb{Z}$, and $\alpha' > \alpha$. As shown in Fig. 2(c), Eq. (20) locates the estimation in much narrower stripes colored in navy, whose width is $1/\alpha' 2^N$. Similarly, the optimal choice of α' should be the maximum value ensuring that there is only one single stripe in the overlap among Eqs. (15), (19), and (20). In other words, we need to keep the distance between new neighbors no less than the width of previous stripes, $1/2^N(2^N - 1)$,

$$\frac{1}{\alpha'} - \frac{1}{2^N \alpha'} \geqslant \frac{1}{2^N(2^N - 1)}. \quad (21)$$

Then the optimal α' is obtained, $\alpha' = (2^N - 1)^2$. Recalling Eq. (19), we can pinpoint $E_j \Delta t/2\pi \hbar$ in a narrower stripe colored in yellow as depicted in Fig. 2(b), whose width is $1/2^N(2^N - 1)^2$, and

$$\frac{E_j \Delta t}{2\pi \hbar} \in \left[\frac{y_j'' - 1/2}{2^N(2^N - 1)^2}, \frac{y_j'' + 1/2}{2^N(2^N - 1)^2} \right], \quad (22)$$

where y_j'' is the corresponding nearest integer.

We can always pick up appropriate α values, and the estimated $E_j \Delta t/2\pi \hbar$ will be pinpointed in narrower slots via QPE with propagators. In other words, more precise estimation is available by repeating the iterative method. In Table I, we present the optimal α values for the iterative method and the corresponding width of the estimated $E_j \Delta t/2\pi \hbar$. The 0th iteration corresponds to the QPE with the original propagator $U_K(\Delta t)$, where $\alpha = 1$. The optimal α is the maximum value guaranteeing that there is only one single stripe in the overlap between the new estimation and the former ones.

We present, in Algorithm 1, the iterative method to improve the precision of the QPE algorithm (QPEA), where ϵ_m is the maximum acceptable additive error, and the optimal α values are applied.

ALGORITHM 1. Algorithm of the iterative QPEA.

Input: Propagator $U_K(\Delta t)$, eigenstate $|\psi_j\rangle$,
    maximum acceptable additive error ϵ_m,
    number of q qubits N.
$\alpha \leftarrow 1$
do QPEA with $U_K(\alpha \Delta t)$, $|\psi_j\rangle$
do Estimate the phase $E_j \Delta t/2\pi \hbar$,
    calculate the additive error ϵ.
while $\epsilon < \epsilon_m$ **do**
    $\alpha \leftarrow (2^N - 1)\alpha$
    do QPEA with $U_K(\alpha \Delta t)$, $|\psi_j\rangle$
    do Estimate the phase $E_j \Delta t/2\pi \hbar$,
        calculate the new additive error ϵ.
end while
Return: Phase $E_j \Delta t/2\pi \hbar$, additive error ϵ.

V. APPLICATION TO THE TWO-SITE HUBBARD MODEL

A simple example can be beneficial to showcase the strengths of the proposed iterative method. Consider the two-site Fermi Hubbard model, whose Hamiltonian is given by [31]

$$H_{\text{hub}} = -t \sum_{\sigma} \left(c_{1,\sigma}^\dagger c_{2,\sigma} + c_{2,\sigma}^\dagger c_{1,\sigma} \right) + u \sum_{j=1,2} n_{i,\uparrow} n_{i,\downarrow}, \quad (23)$$

where t denotes the transfer integral, u denotes the on-site interaction, and $\sigma = \uparrow, \downarrow$ indicates the spin. For simplicity, here we set $\hbar = 1$, and $t = 1, u = 1$. The eigenenergy, eigenstates, and implementation of the propagator can be found in our recent work [32].

Here we focus on the highest-energy state in a half-filling model, corresponding to eigenenergy $E_h = 2.56$. In Figs. 3(a)–3(c), we present the numerical simulation of $\text{Pr}(x)$ for the original QPE with $N = 2, 3, 4$, where $\text{Pr}(x)$ indicates the probability to get result x after measuring the first N qubits, as shown in Eq. (13). The peaks correspond to the
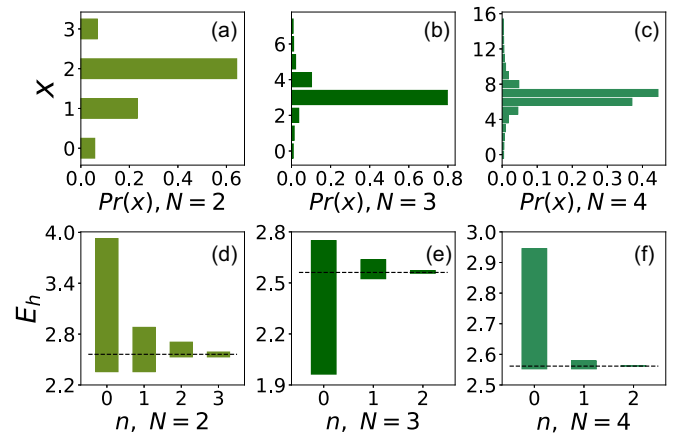

FIG. 3. Numerical simulation results for the standard QPE and the iterative method. (a)–(c) The numerical simulation of $\text{Pr}(x)$ for the original QPE, where $N = 2, 3, 4$ is the number of qubits in the first register of QPE with propagators. (d)–(f) The estimated eigenenergy E_h with the iterative method, where n is the iterative times, and $n = 0$ corresponds to the original QPE.

nearest integer and we can pinpoint the phase term $E_h \Delta t / 2\pi\hbar$ with Eq. (15). In Figs. 3(d)–3(f), we present the estimated eigenenergy E_h with the proposed iterative method, where n is the iterative times, and $n = 0$ corresponds to the standard QPE. With Eqs. (19) and (22), we can pinpoint the eigenenergy E_h in certain ranges as shown in the colored bars in Figs. 3(d)–3(f). The dashed line in Figs. 3(d)–3(f) indicates the exact E_h.

In the standard QPE algorithm, precision is gained by adding more q qubits. Thus, greater N leads to a more precise estimation, corresponding to the $n = 0$ bars in Figs. 3(d)–3(f). In the iterative QPE algorithm, precision is gained in each iteration. The heights of the bars decrease exponentially with the iterative times n in Figs. 3(d)–3(f). More q qubits also leads to higher precision in the iterative QPE algorithm. As shown in Figs. 3(d)–3(f), the heights of the bars decrease more quickly with greater N.

VI. DISCUSSIONS AND CONCLUSIONS

In general, the precision of the final estimation is exponential to the iterative times and N, the number of qubits q. Recalling Eqs. (19) and (22), the additive error of estimated $E_j \Delta t / 2\pi\hbar$ under various iterative times n and number of q qubits N can be given as

$$\epsilon = \frac{C}{2^N(2^N - 1)^n}, \tag{24}$$

where $C \geqslant 1$ is an integer, and in each iteration, we can pinpoint the peak of $\Pr(x)$ in no more than C slots. Ideally, there exists only one single peak slot in $\Pr(x)$ and we can find a single nearest integer, where $C = 1$. However, in a real experiment, due to the existence of noises and imperfect hardware, it is often difficult to find out the exact single peak slot of $\Pr(x)$. An example is as shown in Fig. 3(c), where $\Pr(x = 7)$ is the peak in the numerical simulation, yet $\Pr(x = 6)$ is very close to $\Pr(x = 7)$. In experiment, due to noises and errors, one might find a plateau covering $\Pr(x = 6)$ and $\Pr(x = 7)$, and have to include both slots in the estimation.

In Fig. 4, we present the width of estimated $E_j \Delta t / 2\pi\hbar$ under various iterative times and number of q qubits, where we always apply the optimal α in iteration. We notice that high precision is available by the iterative method, even though there are only two or three q qubits as ancilla qubits, as shown in Figs. 3(d) and 3(e). Thus, the iterative QPE with propagators is a promising approach toward precise estimations on NISQ devices, where it is often challenging to implement QPE
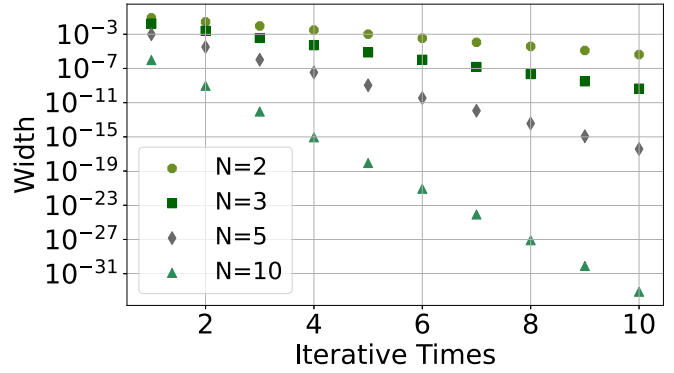

FIG. 4. Width of estimated $\frac{E_j \Delta t}{2\pi\hbar}$ under various iterative times and number of q qubits. N is the number of qubits in the first register of QPE with propagators. Here we apply the optimal α in each iteration.

among too many qubits due to the existence of noises and limitation of connections.

However, the iterative method is hardly feasible for the original QPE with given operator U. Here we focus on QPE with propagators, corresponding to a unitary operator $U_K(\Delta t)$. In the iteration, for certain α value, we do not directly implement $U_K(\Delta t)^\alpha$, yet we instead apply $U_K(\alpha \Delta t)$, which is still a single unitary operator. Therefore, the depth of the quantum circuit does not change in the iteration. However, if the given unitary operator U in the original QPE is replaced as U^α, the new quantum circuit can be considerably deeper, which can be extremely challenging to implement on NISQ devices.

In conclusion, we propose an iterative method to improve the precision of QPE. We revisit the original QPE, and QPE with propagator enables us to pinpoint the phase corresponding to an eigenenergy in a certain range. QPE with propagators over longer time spans can lead to "comblike" estimations, with which we are able to pinpoint the same estimation in a branch of discrete narrower ranges. Thus, by applying iterative QPE with propagators over a variety of time spans, we are able to pinpoint the estimation more precisely. High precision is available by the iterative method, even if there are only a few qubits as ancilla qubits. The iterative QPE with propagators provides a feasible and promising approach to estimate the corresponding eigenvalue more precisely on NISQ devices.

ACKNOWLEDGMENT

[1] R. P. Feynman, Simulating physics with computers, Intl. J. Theor. Phys. **21**, 467 (2018).

[2] F. Arute, K. Arya, R. Babbush, D. Bacon, J. C. Bardin, R. Barends, R. Biswas, S. Boixo, F. G. Brandao, D. A. Buell *et al.*, Quantum supremacy using a programmable superconducting processor, Nature (London) **574**, 505 (2019).

[3] H.-S. Zhong, H. Wang, Y.-H. Deng, M.-C. Chen, L.-C. Peng, Y.-H. Luo, J. Qin, D. Wu, X. Ding, Y. Hu *et al.*, Quantum computational advantage using photons, Science **370**, 1460 (2020).

[4] E. Altman, K. R. Brown, G. Carleo, L. D. Carr, E. Demler, C. Chin, B. DeMarco, S. E. Economou, M. A. Eriksson, Kai-Mei C. Fu *et al.*, Quantum simulators: Architectures and opportunities, PRX Quantum **2**, 017003 (2021).

[5] Y. Kim, A. Eddins, S. Anand, K. X. Wei, E. Van Den Berg, S. Rosenblatt, H. Nayfeh, Y. Wu, M. Zaletel, K. Temme *et al.*, Evidence for the utility of quantum computing before fault tolerance, Nature (London) **618**, 500 (2023).

[6] A. D. King, J. Raymond, T. Lanting, R. Harris, A. Zucca, F. Altomare, A. J. Berkley, K. Boothby, S. Ejtemaee, C. Enderud *et al.*, Quantum critical dynamics in a 5000-qubit programmable spin glass, Nature (London) **617**, 61 (2023).

[7] J. Biamonte, P. Wittek, N. Pancotti, P. Rebentrost, N. Wiebe, and S. Lloyd, Quantum machine learning, Nature (London) **549**, 195 (2017).

[8] S. Bravyi, D. Gosset, and R. König, Quantum advantage with shallow circuits, Science **362**, 308 (2018).

[9] S. Boixo, S. V. Isakov, V. N. Smelyanskiy, R. Babbush, N. Ding, Z. Jiang, M. J. Bremner, J. M. Martinis, and H. Neven, Characterizing quantum supremacy in near-term devices, Nat. Phys. **14**, 595 (2018).

[10] I. Cong, S. Choi, and M. D. Lukin, Quantum convolutional neural networks, Nat. Phys. **15**, 1273 (2019).

[11] M. Sajjan, J. Li, R. Selvarajan, S. H. Sureshbabu, S. S. Kale, R. Gupta, V. Singh, and S. Kais, Quantum machine learning for chemistry and physics, Chem. Soc. Rev. **51**, 6475 (2022).

[12] A. Y. Kitaev, Quantum measurements and the Abelian stabilizer problem, arXiv:quant-ph/9511026.

[13] P. W. Shor, Polynomial-time algorithms for prime factorization and discrete logarithms on a quantum computer, SIAM Rev. **41**, 303 (1999).

[14] A. W. Harrow, A. Hassidim, and S. Lloyd, Quantum algorithm for linear systems of equations, Phys. Rev. Lett. **103**, 150502 (2009).

[15] E. Farhi, J. Goldstone, S. Gutmann, and M. Sipser, Quantum computation by adiabatic evolution, arXiv:quant-ph/0001106.

[16] A. Aspuru-Guzik, A. D. Dutoi, P. J. Love, and M. Head-Gordon, Simulated quantum computation of molecular energies, Science **309**, 1704 (2005).

[17] B. P. Lanyon, J. D. Whitfield, G. G. Gillett, M. E. Goggin, M. P. Almeida, I. Kassal, J. D. Biamonte, M. Mohseni, B. J. Powell, M. Barbieri *et al.*, Towards quantum chemistry on a quantum computer, Nat. Chem. **2**, 106 (2010).

[18] P. J. J. O'Malley, R. Babbush, I. D. Kivlichan, J. Romero, J. R. McClean, R. Barends, J. Kelly, P. Roushan, A. Tranter, N. Ding, B. Campbell, Y. Chen, Z. Chen, B. Chiaro, A. Dunsworth, A. G. Fowler, E. Jeffrey, E. Lucero, A. Megrant, J. Y. Mutus, M. Neeley, C. Neill, C. Quintana, D. Sank, A. Vainsencher, J.

Wenner, T. C. White, P. V. Coveney, P. J. Love, H. Neven, A. Aspuru-Guzik, and J. M. Martinis, Scalable quantum simulation of molecular energies, Phys. Rev. X **6**, 031007 (2016).

[19] P. M. Cruz, G. Catarina, R. Gautier, and J. Fernández-Rossier, Optimizing quantum phase estimation for the simulation of Hamiltonian eigenstates, Quantum Sci. Technol. **5**, 044005 (2020).

[20] B. Bauer, S. Bravyi, M. Motta, and G. K.-L. Chan, Quantum algorithms for quantum chemistry and quantum materials science, Chem. Rev. **120**, 12685 (2020).

[21] M. Motta, C. Sun, A. T. Tan, M. J. O'Rourke, E. Ye, A. J. Minnich, F. G. Brandao, and G. K.-L. Chan, Determining eigenstates and thermal states on a quantum computer using quantum imaginary time evolution, Nat. Phys. **16**, 205 (2020).

[22] J. Preskill, Quantum computing in the NISQ era and beyond, Quantum **2**, 79 (2018).

[23] H. Mohammadbagherpoor, Y.-H. Oh, A. Singh, X. Yu, and A. J. Rindos, Experimental challenges of implementing quantum phase estimation algorithms on IBM quantum computer, arXiv:1903.07605.

[24] J. D. Whitfield, J. Biamonte, and A. Aspuru-Guzik, Simulation of electronic structure Hamiltonians using quantum computers, Mol. Phys. **109**, 735 (2011).

[25] P. Jordan and E. Wigner, About the Pauli exclusion principle, Z. Phys. **47**, 631 (1928).

[26] R. Somma, G. Ortiz, J. E. Gubernatis, E. Knill, and R. Laflamme, Simulating physical phenomena by quantum networks, Phys. Rev. A **65**, 042323 (2002).

[27] N. Hatano and M. Suzuki, Finding exponential product formulas of higher orders, *Quantum Annealing and Other Optimization Methods* (Springer, New York, 2005), pp. 37–68.

[28] R. P. Feynman, Space-time approach to nonrelativistic quantum mechanics, Rev. Mod. Phys. **20**, 367 (1948).

[29] S. Lloyd, Universal quantum simulators, Science **273**, 1073 (1996).

[30] R. Cleve, A. Ekert, C. Macchiavello, and M. Mosca, Quantum algorithms revisited, Proc. R. Soc. London A **454**, 339 (1998).

[31] J. Hubbard, Electron correlations in narrow energy bands, Proc. R. Soc. London A **276**, 238 (1963).

[32] J. Li, B. A. Jones, and S. Kais, Toward perturbation theory methods on a quantum computer, Sci. Adv. **9**, eadg4576 (2023).